

Structure and electrochemical properties of $\text{Li}(\text{Ni}_{0.5}\text{Mn}_{0.5})_{1-x}\text{Ti}_x\text{O}_2$ prepared by one-step solid state reaction

CAO Si-hai(曹四海)¹, WANG Zhi-xing(王志兴)¹, LI Xin-hai(李新海)¹,
GUO Hua-jun(郭华军)¹, PENG Wen-jie(彭文杰)¹, YIN Zhou-lan(尹周澜)²

1. School of Metallurgical Science and Engineering, Central South University, Changsha 410083, China;
2. School of Chemistry and Chemical Engineering, Central South University, Changsha 410083, China

Received 5 January 2006; accepted 31 March 2006

Abstract: The layered compound $\text{Li}(\text{Ni}_{0.5}\text{Mn}_{0.5})_{1-x}\text{Ti}_x\text{O}_2$ powders were prepared with $\text{Ni}(\text{OH})_2$, MnCO_3 , Li_2CO_3 and TiO_2 by one-step solid state reaction. The effect of doping Ti on the structure and electrochemical properties was studied. The XRD results indicate that the powders with $0 \leq x \leq 0.05$ have good layered structure and trace of impurity appears in the samples with $x \geq 0.1$. The SEM photographs show that the particle size distributes homogeneously and the sample with $x=0.15$ has larger particle size than other samples. The charge-discharge tests show that $\text{Li}(\text{Ni}_{0.5}\text{Mn}_{0.5})_{0.95}\text{Ti}_{0.05}\text{O}_2$ synthesized at 800 °C for 36 h exhibits good electrochemical properties. It firstly delivers 173 mA·h/g and maintains 90% of the initial discharge capacity after 30 cycles. The cyclic voltammetry and differential capacity vs voltage curves show that the major oxidation and reduction peaks are around 3.95 V and 3.75 V, respectively, assigned to $\text{Ni}^{2+}/\text{Ni}^{4+}$ oxidation-reduction process. A weak peak around 4.5 V is found during the oxidation process in the first cycle, which can be regarded as the main reason of the large drop of discharge capacity in the initial cycle.

Key words: Li-ion battery; cathode; $\text{LiNi}_{0.5}\text{Mn}_{0.5}\text{O}_2$; doping; Ti; cyclic voltammetry

1 Introduction

Many efforts have been made to develop new materials as an alternative to LiCoO_2 due to the relatively high cost and toxicity of Co. Since OHZUKU and MAKIMURA[1] successfully synthesized $\text{LiNi}_{0.5}\text{Mn}_{0.5}\text{O}_2$ with excellent performance by solid state reaction at 1 000 °C, $\text{LiNi}_{0.5}\text{Mn}_{0.5}\text{O}_2$ has attracted much attention from researchers in view of its high reversible capacity, high thermal stability, lower cost and less toxicity. Simultaneously LU et al[2] synthesized a series of layered $\text{Li}[\text{Ni}_x\text{Li}_{(1/3-2x/3)}\text{Mn}_{(2/3-x/3)}]\text{O}_2$ using mixed hydroxide method. XPS studies showed that the transition metal elements are predominantly in Ni^{2+} and Mn^{4+} oxidation state and 6%–8% of Ni- and Mn-ions in the compound are in mixed valence state due to the dynamic ion-equilibrium, $\text{Ni}^{2+}+\text{Mn}^{4+} \rightleftharpoons \text{Ni}^{3+}+\text{Mn}^{3+}$ [3]. The Ni and Mn K-edge X-ray absorption near-edge structure(XANES) study on $\text{LiNi}_{0.5}\text{Mn}_{0.5}\text{O}_2$ is also in agreement with that Ni and Mn ions are predominantly 2+ and 4+ oxidation states[4]. A two-electron redox

reaction ($\text{Ni}^{2+} \rightleftharpoons \text{Ni}^{4+}$) is assumed for the charge-discharge process and confirmed by XANES up to 4.2 V in $\text{LiNi}_{0.5}\text{Mn}_{0.5}\text{O}_2$ [3–5].

It was reported that an electrochemically inactive component Li_2MnO_3 , notated as $\text{Li}[\text{Li}_{1/3}\text{Mn}_{2/3}]\text{O}_2$ can stabilize the structure of $\text{LiNi}_{0.5}\text{Mn}_{0.5}\text{O}_2$ and suppress the transformation of the layered $\text{LiNi}_{0.5}\text{Mn}_{0.5}\text{O}_2$ to a spinel structure[6]. When $x\text{Li}_2\text{MnO}_3 \cdot (1-x)\text{LiMO}_2$ electrodes are initially charged to a high potential, typically above 4.5V (vs Li/Li^+), lithia(Li_2O) is extracted from the Li_2MnO_3 component in a combined electrochemical process (lithium removal) and chemical process (oxygen loss) before electrolyte oxidation[7]. This initial reaction is coulombically inefficient and the discharge capacity can be 20%–30% less than the charge capacity. In the previous study we have successfully synthesized the layered $\text{LiNi}_{0.5}\text{Mn}_{0.5}\text{O}_2$ with $\text{Ni}(\text{OH})_2$, MnCO_3 and Li_2CO_3 as starting materials by one step solid-state reaction without preheating process. However the cycling performance of the sample still needs to be improved. We think the loss of capacity relates to the coulombically inefficient reaction of Li_2MnO_3 which

was confirmed to exist in the electrode from the XRD pattern and the loss of oxygen at the surface of electrode with high charged state. JOHNSON et al[8] reported that Li_2TiO_3 can decrease the activity of oxygen on the surface of delithiated electrode at high charge stages. And KANG et al[9] reported that doping Al, Ti and Co increased the discharge capacity and electrochemical conductivity of $\text{LiNi}_{0.5}\text{Mn}_{0.5}\text{O}_2$. Therefore we intend to synthesize $\text{Li}(\text{Ni}_{0.5}\text{Mn}_{0.5})_{1-x}\text{Ti}_x\text{O}_2$ with conventional solid-state reaction to improve its electrochemical properties. The effect of doping Ti on the structure and electrochemical properties of $\text{Li}(\text{Ni}_{0.5}\text{Mn}_{0.5})_{1-x}\text{Ti}_x\text{O}_2$ with different x is systematically studied.

2 Experimental

The stoichiometrical $\text{Ni}(\text{OH})_2$, MnCO_3 , Li_2CO_3 and TiO_2 were thoroughly mixed according to the formula of $\text{Li}(\text{Ni}_{0.5}\text{Mn}_{0.5})_{1-x}\text{Ti}_x\text{O}_2$ ($x=0, 0.02, 0.05, 0.10, 0.15$) and ground for 6 h with a ball mill. The ground powder was heated at 800 °C in air for 36 h and then cooled naturally to room temperature in furnace.

The powder X-ray diffraction (Rigaku, Rint-2000) with $\text{CuK}\alpha$ radiation was used to identify the crystalline phase of the as-prepared powders at a scanning rate of $2^\circ/\text{min}$. The scanning electron microscopy (SEM) study of the powders was performed on JEOL JSM-5600LV electron microscope.

The charge/discharge tests were carried out using the CR2025 coin-type cell, which consisted of a cathode and lithium metal anode separated by a Celgard 2400 porous polypropylene film with the electrolyte of 1 mol/L LiPF_6 in EC+DMC+EMC(1:1:1, volume ratio). The positive electrode consisted of oxide powder, acetylene balck and PVDF at a ratio of 80:10:10. The cathode mixture was thoroughly mixed, then coated on an aluminum mesh current collector and dried at 120 °C for 12 h under vacuum. The cells were assembled in a glove box filled with dried argon gas. The cells were first charged to 4.5 V at a rate of 20 mA/g and held for 2 h under 4.5 V, then discharged to 2.5 V at a rate of 20 mA/g.

The cyclic voltammetry study was carried out by means of tri-electrode cell, using lithium metal as counter and reference electrodes. The cell was operated at a scan rate of 0.05 mV/s (vs Li/Li^+) in the voltage range of 2.5–4.7 V at room temperature. The differential capacity vs voltage study was operated on the coin cell from 2.5 V to 4.7 V. The fresh assembled cells were set for several hours before tests.

3 Results and discussion

The XRD patterns of $\text{Li}(\text{Ni}_{0.5}\text{Mn}_{0.5})_{1-x}\text{Ti}_x\text{O}_2$ powder

synthesized with different value of x are shown in Fig. 1. All peaks are sharp and well defined for materials with $0 \leq x \leq 0.05$, which demonstrates that the compounds are well crystallized and indexed to $\alpha\text{-NaFeO}_2$ layered structure with space group of $R\bar{3}m$. The peaks marked with # between 20° and 25° caused by superlattice ordering of Li, Ni and Mn in the 3a site indicate a layered structure with Li_2MnO_3 character (space group: $C2/m$)[10,11]. According to Ref.[6], Li_2MnO_3 contributes to the structural stabilization of $\text{LiNi}_{0.5}\text{Mn}_{0.5}\text{O}_2$ material during the cycling process of electrode materials. With the increase of x , the diffraction intensity of Li_2MnO_3 increases because of the appearance of Li_2TiO_3 which has isostructure with Li_2MnO_3 [12]. Meanwhile, the split degree for peaks (018) and (110) becomes more obvious, which demonstrates that the materials have more integrated layered structure. And all diffraction peaks shift toward lower angle, which demonstrates the lattice parameters changed. Peaks (marked with *) of some uncertain impurity appear when $x=0.10$ and become more obvious for $x=0.15$. The lattice parameters are shown in Table 1. It is clear that a axis shrinks and c axis expands with the increase of x when $0 \leq x \leq 0.05$. The ratio of c/a also increases and is above 4.936, which is in good agreement with layered structure. The change of lattice parameters may be related to the partial substitution of Ni^{2+} ($r=0.69 \text{ \AA}$) and Mn^{4+} ($r=0.53 \text{ \AA}$) by Ti^{4+} ($r=0.68 \text{ \AA}$). The increasing ratio of I_{003}/I_{104} suggests that the degree of cation mixing becomes less severe, which means that less Ni^{2+} and Li^+ ions interchange their sites in the layered structure[1,13].

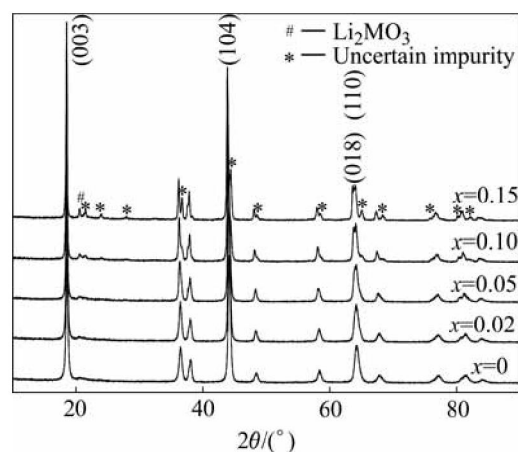


Fig.1 XRD patterns of synthesized $\text{Li}(\text{Ni}_{0.5}\text{Mn}_{0.5})_{1-x}\text{Ti}_x\text{O}_2$

Table 1 Lattice parameters of $\text{Li}(\text{Ni}_{0.5}\text{Mn}_{0.5})_{1-x}\text{Ti}_x\text{O}_2$

| $\text{Li}(\text{Ni}_{0.5}\text{Mn}_{0.5})_{1-x}\text{Ti}_x\text{O}_2$ | $a/\text{\AA}$ | $c/\text{\AA}$ | c/a | I_{003}/I_{104} |
|------------------------------------------------------------------------|----------------|----------------|-------|-------------------|
| $x=0$ | 2.885 | 14.242 | 4.937 | 0.962 |
| $x=0.02$ | 2.884 | 14.243 | 4.939 | 1.017 |
| $x=0.05$ | 2.883 | 14.252 | 4.944 | 1.067 |
| $x=0.10$ | 2.883 | 14.244 | 4.941 | 1.157 |
| $x=0.15$ | 2.873 | 14.265 | 4.966 | 1.229 |

Fig.2 shows the SEM photographs for $\text{Li}(\text{Ni}_{0.5}\text{Mn}_{0.5})_{1-x}\text{Ti}_x\text{O}_2$ synthesized with different x . All samples have homogeneous particle size distribution. The average particle size of samples with $0 \leq x \leq 0.10$ is about 200 nm. The difference of the morphology is not obvious except for the sample with $x=0$ (Fig.2(a)). However the particle size increases quickly (Fig.2(e)) when $x=0.15$, which maybe relates to the existence of great amount of impurity. The particles with large size would hinder the diffusion of lithium ions between particles, and then influence the electrochemical performance of the sample, which will be discussed later.

The first charge-discharge curves of synthesized samples with different x are shown in Fig.3. The samples with $x=0, 0.02, 0.05, 0.10, 0.15$ deliver the capacities of 176, 186, 173, 140 and 84 mA·h/g, respectively. It can be seen that a slight amount ($x \leq 0.02$) of dopant TiO_2 evidently increases the discharge capacity, which may be related to the increase of electrical conductivity of materials after doping. However, the first discharge capacity decreases rapidly with the increase of x when

$x \geq 0.05$, which is due to the decrease of the theoretical capacity of $\text{Li}(\text{Ni}_{0.5}\text{Mn}_{0.5})_{1-x}\text{Ti}_x\text{O}_2$ with the increasing amount of electrochemically inactive dopant TiO_2 . The cathode material with $x=0.15$ shows larger polarization than others because larger particles expand the diffusion distance between particles.

The cycling performance of the samples is shown in Fig.4. The samples with $x=0, 0.02, 0.05, 0.10, 0.15$ retain 75%, 78%, 90%, 99%, 134% of the initial discharge capacity respectively after 30 cycles between 2.5 V and 4.5 V at a current of 20 mA/g. It is obvious that the samples have better cycling performance with the increase of x , which may be related to the decrease of activity of oxygen at the surface of delithiated electrode at high charge stages. In addition, it also relates to more stable layered structure of materials after doping Ti because $\text{Ti}-\text{O}$ (470.4 kJ/mol) has more strong bond energy compared with $\text{Ni}-\text{O}$ (391.6 kJ/mol) and $\text{Mn}-\text{O}$ (402.34 kJ/mol). The similar doping effect of Ti substitution for the Mn site was already reported elsewhere[14]. However, the reversible capacity of

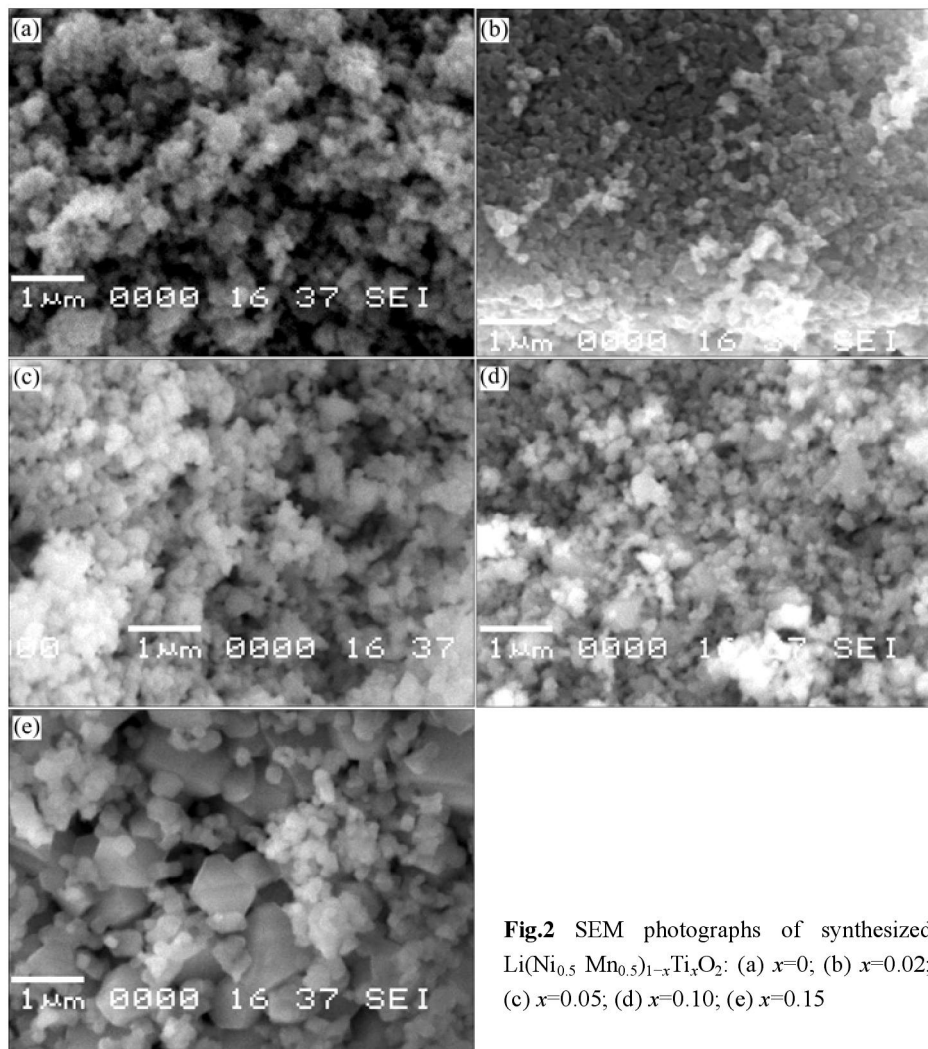


Fig.2 SEM photographs of synthesized $\text{Li}(\text{Ni}_{0.5}\text{Mn}_{0.5})_{1-x}\text{Ti}_x\text{O}_2$: (a) $x=0$; (b) $x=0.02$; (c) $x=0.05$; (d) $x=0.10$; (e) $x=0.15$

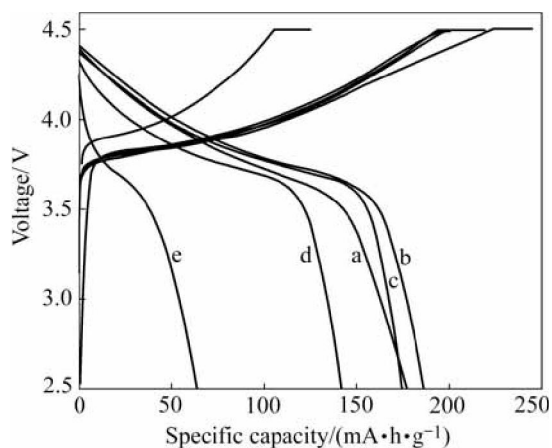


Fig.3 First discharge curves of synthesized samples $\text{Li}(\text{Ni}_{0.5}\text{Mn}_{0.5})_{1-x}\text{Ti}_x\text{O}_2$: (a) $x=0$; (b) $x=0.02$; (c) $x=0.05$; (d) $x=0.10$; (e) $x=0.15$

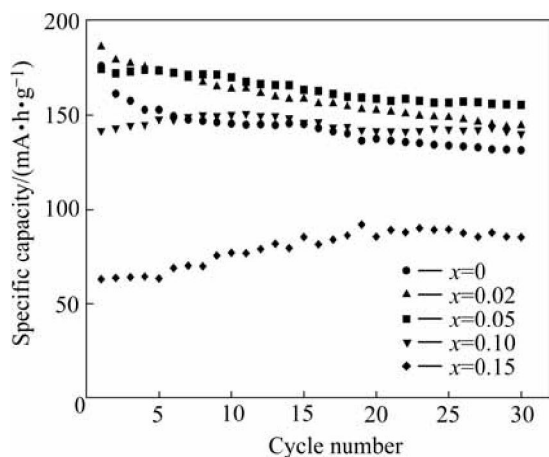


Fig.4 Cycling performance curves of synthesized samples $\text{Li}(\text{Ni}_{0.5}\text{Mn}_{0.5})_{1-x}\text{Ti}_x\text{O}_2$ cycled between 2.5 V and 4.5 V at current of 20 mA/g

samples with $x \geq 0.10$ decreases rapidly compared with other samples due to the decrease of theoretical capacity. During the cycling process the reversible capacity for samples with $x=0.10$, 0.15 firstly increases and then decreases, which may relate to the difficult activation of samples with large particles.

In order to understand the reason for the large drop of discharge capacity for $\text{Li}(\text{Ni}_{0.5}\text{Mn}_{0.5})_{0.98}\text{Ti}_{0.02}\text{O}_2$ in the first cycle, the cyclic voltammograms (CV) and differential capacity voltage tests were carried out. The CV curves of $\text{Li}(\text{Ni}_{0.5}\text{Mn}_{0.5})_{0.98}\text{Ti}_{0.02}\text{O}_2$ cell between 2.5 V and 4.7 V for the first three cycles at room temperature are shown in Fig.5. It is clear that the major oxidation and reduction peaks are observed at around 3.95 V (4.0 V for the first cycle) and 3.75 V respectively. These two observed peaks can be assigned to $\text{Ni}^{2+}/\text{Ni}^{4+}$ oxidation-reduction redox. Obvious difference can be observed between the first cycle and the following two cycles. For the oxidation process of the first cycle, an

additional weak peak around 4.5 V is observed, yet disappears in the following cycles. All these can also be seen from the differential capacity vs voltage curves in Fig.6. The similar oxidation peak around 4.5 V was also reported in other Refs.[12,15]. However there is still no related report about the origin of this weak peak. It was reported that a plateau near 4.5 V appeared in $\text{Li}_y\text{Mn}_x\text{Ni}_{1-x}\text{O}_2$ prepared by solid state method, which means the presence of NiO[16]. However, there is no existence of the plateau near 4.5 V in the charge curves in Fig.3. From the difference of curves of different cycles in Fig.5 and Fig.6, it is suggested that the oxidation peak around 4.5 V is the main reason for the large capacity drop of $\text{Li}(\text{Ni}_{0.5}\text{Mn}_{0.5})_{0.98}\text{Ti}_{0.02}\text{O}_2$ after the first cycle. The origin of this oxidation peak probably is related to the coulombically inefficient reaction of Li_2MnO_3 under high voltage[7].

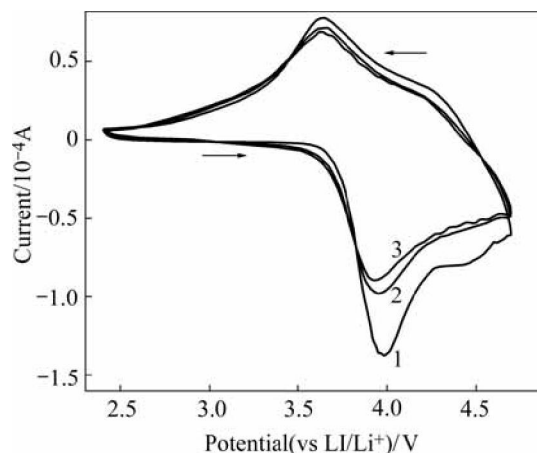


Fig.5 Cyclic voltammogram (CV) curves of $\text{Li}(\text{Ni}_{0.5}\text{Mn}_{0.5})_{0.98}\text{Ti}_{0.02}\text{O}_2$

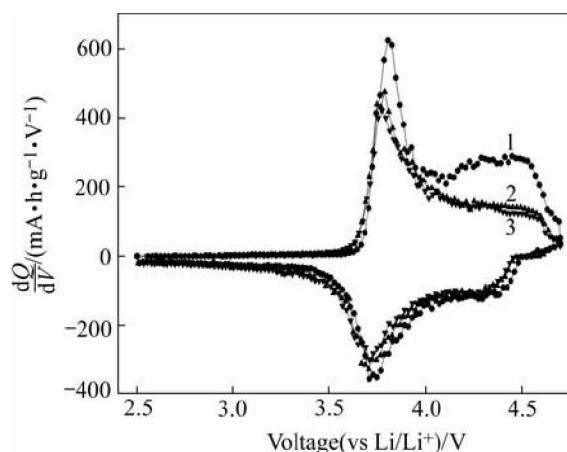


Fig.6 Differential capacity vs voltage curves of $\text{Li}(\text{Ni}_{0.5}\text{Mn}_{0.5})_{0.98}\text{Ti}_{0.02}\text{O}_2$

4 Conclusions

The layered compound $\text{Li}(\text{Ni}_{0.5}\text{Mn}_{0.5})_{1-x}\text{Ti}_x\text{O}_2$ was prepared by one step solid-state reaction with $\text{Ni}(\text{OH})_2$,

MnCO₃, Li₂CO₃ and TiO₂. The XRD results indicate that the powders with $0 \leq x \leq 0.05$ have good layered structure. The SEM photographs show the particle size distributes homogeneously. The Li(Ni_{0.5}Mn_{0.5})_{0.95}Ti_{0.05}O₂ synthesized at 800 °C for 36 h exhibits good electrochemical properties. It firstly delivers 173 mA·h/g and retains 90% of the initial discharge capacity after 30 cycles. During the charge-discharge electrochemical process the major oxidation and reduction peaks are around 3.95 V (4.0 V for the first cycle) and 3.75 V respectively, which can be assigned to Ni²⁺/Ni⁴⁺ oxidation-reduction process. The weak peak around 4.5 V during the oxidation process in the first cycle can be regarded as the main reason of the large drop of discharge capacity in the initial cycles.

References

- [1] OHZUKU T, MAKIMURA Y. Layered lithium insertion material of LiNi_{1/2}Mn_{1/2}O₂: A possible alternative to LiCoO₂ for advanced lithium-ion batteries [J]. Chem Lett, 2001, 8: 744–745.
- [2] LU Z H, MACNEIL D D, DAHN J R. Layered cathode materials Li[Ni_xLi_(1/3-2x/3)Mn_(2/3-x/3)]O₂ for lithium-ion batteries [J]. Electrochem Solid State Lett, 2001, 4(11): A191–A194.
- [3] SHAJU K M, RAO G V S, CHOWDARI B V R. X-ray photoelectron spectroscopy and electrochemical behaviour of 4 V cathode, Li(Ni_{1/2}Mn_{1/2})O₂ [J]. Electrochim Acta, 2003, 48: 1505–1514.
- [4] JOHNSON C S, KIM J S, KOENE L. The role of Li₂MO₂ structures (M=metal ion) in the electrochemistry of (x)LiMn_{0.5}Ni_{0.5}O₂(1-x)-Li₂TiO₃ electrodes for lithium-ion batteries [J]. Electrochem Commun, 2002(4): 492–498.
- [5] YOON W S, PAIK Y, YANG X Q, BALASUBRAMANIAN M, MCBREEN J, GREY C P. Investigation of the local structure of the LiNi_{0.5}Mn_{0.5}O₂ cathode material during electrochemical cycling by X-ray absorption and NMR spectroscopy [J]. Electrochem Solid State Lett, 2002, 5(11): A263–A266.
- [6] KIM J H, SUNY K. Electrochemical performance of Li[Li_xNi_{(1-3x)/2}Mn_{(1+x)/2}]O₂ cathode materials synthesized by a sol-gel method [J]. Journal of Power Sources, 2003, 119/121: 166–170.
- [7] KIM J S, JOHNSON C S, VAUGHY J T, THACKERAY M M, HACKNEY S A, YOON W, GREY C P. Electrochemical and structural properties of x Li₂M'O₃(1-x)LiMn_{0.5}Ni_{0.5}O₂ electrodes for lithium batteries (M'=Ti, Mn, Zr; 0≤x≤0.3) [J]. Chem Mater, 2004, 16: 1996–2006.
- [8] JOHNSON C S, KIM J S, KROPF A J, KAHAIAN A J, VAUGHY J T, THACKERAY M M. Structure and electrochemical evaluation of (1-x)Li₂TiO₃(x)LiNi_{0.5}Mn_{0.5}O₂ electrodes for lithium batteries [J]. J Power Sources, 2003, 119/121: 139–144.
- [9] KANG S H, KIM J, STOLL M E, ABRAHAM D, SUN Y K, AMINE K. Layered Li(Ni_{0.5-x}Mn_{0.5-x}M'_{2x})O₂(M'=Co, Al, Ti; x=0, 0.025) cathode materials for Li-ion rechargeable batteries [J]. J Power Sources, 2002, 112: 41–48.
- [10] LU Z H, BEAULIEU L Y, DONABERGER R A, THOMAS C L, DAHN J R. Synthesis structure, and electrochemical behavior of Li[Ni_xLi_(1/3-2x/3)Mn_(2/3-x/3)]O₂ [J]. J Electrochem Soc, 2002, 149: A778–A791.
- [11] LU Z H, DAHN J R. In situ and ex situ XRD investigation of Li[Cr_xLi_(1/3-x/3)Mn_(2/3-2x/3)]O₂ (x=1/3) cathode material [J]. J Electrochem Soc, 2003, 150: A1044–A1051.
- [12] JIM J S, JOHNSON C S, THACKERAY M M. Layered xLiMO₂(1-x)Li₂MnO₃ electrodes for lithium batteries: A study of 0.95LiNi_{0.5}Mn_{0.5}O₂·0.05Li₂TiO₃ [J]. Electrochem Commun, 2002, 4: 205–209.
- [13] OHZUKU T, UEDA A, NAGAYAMA M. Electrochemistry and structural chemistry of LiNiO₂ (R3m) for 4 volt secondary lithium cells [J]. J Electrochem Soc, 1993, 140: 1862–1870.
- [14] MYUNG S T, KOMABA S, HOSOYA K, HIROSAKI N, MIURA Y, KUMAGAI N. Synthesis of LiNi_{0.5}Mn_{0.5-x}Ti_xO₂ by an emulsion drying method and effect of Ti on structure and electrochemical properties [J]. Chem Mater, 2005, 17(9): 2427–2435.
- [15] LI D, MUTA T, NOGUCHI H. Electrochemical characteristics of LiNi_{0.5}Mn_{0.5-x}Ti_xO₂ [J]. J Power Sources, 2004, 135: 262–266.
- [16] YOSHIO M, TODOROV Y, YAMATO K, NOGUCHI H, ITOH J, OKADA M, MOURI T. Preparation of Li₃Mn_xNi_{1-x}O₂ as a cathode for lithium-ion batteries [J]. J Power Sources, 1998, 74: 46–53.

(Edited by YUAN Sai-qian)